

Disintegration of Microcrystalline $\text{Zn}_2\text{SiO}_4\text{:Mn}$ Phosphor Powder

K. A. Petrovykh^{a,b}, A. A. Rempel^{a,b}, V. S. Kortov^b, A. A. Valeeva^{a,b}, and S. V. Zvonarev^b

^a Institute of Solid State Chemistry, Ural Branch, Russian Academy of Sciences,
Pervomaiskaya ul. 91, Yekaterinburg, 620041 Russia

^b Yeltsin Federal University, ul. Mira 19, Yekaterinburg, 620002 Russia

e-mail: kspetrovykh@mail.ru

Received March 18, 2013

Abstract— $\text{Zn}_2\text{SiO}_4\text{:Mn}$ (willemite) nanoparticles ~30 nm in size have been prepared by disintegrating microcrystalline willemite powder in a planetary ball mill. X-ray diffraction and scanning electron microscopy characterization showed that ball milling of the $\text{Zn}_2\text{SiO}_4\text{:Mn}$ powder for 60 min or a longer time ensured complete disintegration of the microcrystalline material and that the crystal structure of the resultant nanoparticles was identical to that of the parent powder.

DOI: 10.1134/S0020168513100087

INTRODUCTION

Microcrystalline $\text{Zn}_2\text{SiO}_4\text{:Mn}$ (willemite) with a crystal size in the range 20–40 μm is widely used as a cathodoluminescent phosphor with a bright green emission band in cathode ray tubes, field-emission and plasma display screens, and other products. The crystal structure of this compound was described as early as 1926 by Zachariasen [1] and refined later by Simonov et al. [2].

$\text{Zn}_2\text{SiO}_4\text{:Mn}$ (willemite) is known to crystallize in trigonal symmetry. The zinc and silicon ions in its structure are in tetrahedral oxygen coordination. Substitution of manganese (Mn^{2+}) ions for zinc (Zn^{2+}) ions gives rise to bright green luminescence even when the Mn^{2+} content of willemite is within tenths of an atomic percent. The peak emission wavelength is typically about 520 nm, which corresponds to the $^4T_1 \rightarrow ^6A_1$ electronic transition. Since this radiative transition is spin-forbidden, the luminescence has a relatively long decay time; that is, willemite exhibits bright phosphorescence [3].

There is currently a need for nanocrystalline phosphors, which have a number of obvious advantages over single-crystalline materials. Reducing the particle size to a nanoscale level considerably improves the radiation hardness of the material [4], which allows one to increase the working power density of the excitation electron beam and, accordingly, the emission brightness. Moreover, the adhesion between a nanophosphor and substrates increases by an order of magnitude, extending the device life by several times [5].

One of the simplest and most effective ways of producing nanomaterials is disintegration through high-energy milling in planetary, vibratory, and ball mills. Using this approach, a coarse-grained material can be converted to nanopowder with an average particle size from 100 to 10 nm. In particular, ball milling was used

to obtain vanadium monoxide and tungsten carbide nanopowders with a particle size near 20 nm [6, 7].

In this paper, we describe the disintegration of microcrystalline $\text{Zn}_2\text{SiO}_4\text{:Mn}$ phosphor powder and the preparation of nanopowders with different particle sizes.

EXPERIMENTAL

Microcrystalline willemite powder was disintegrated in a Retsch PM 200 planetary ball mill using grinding media and vials coated with yttria-stabilized zirconia. The ball-to-powder weight ratio was 10 : 1. To obtain fine powder, isopropanol, $\text{CH}_3\text{CH}(\text{OH})\text{CH}_3$, was used as the milling liquid. After milling, the powders were dried.

The milling process had the following parameters: rotation speed of the supporting disk, 500 rpm; milling time of 15, 30, 60, 120, and 240 min; rotation direction reversed every 5 min at milling times of 15 and 30 min and every 15 min at milling times of 60 min or longer; interval between direction reversals, 5 s.

To relieve the milling-induced stress and remove some of the adsorbate, the powders milled for more than 60 min were annealed in air for 2 h. To prevent particle growth, the annealing temperature was chosen to meet the relation $T \leq 0.3T_m$, where T_m is the melting point of the material [8]. T_{ann} was 573 K.

The as-prepared and milled willemite powders were characterized by X-ray diffraction on a Shimadzu XRD-7000 diffractometer ($\text{CuK}_{\alpha 1,2}$ radiation, angular range $2\theta = 15^\circ$ to 95° , step-scan mode with a step $\Delta(2\theta) = 0.02^\circ$ and a counting time per data point of 10 s). The instrumental broadening of diffraction peaks (the resolution function of the diffractometer) was determined in a special experiment using a lanthanum hexaboride, LaB_6 , powder standard (NIST Stan-

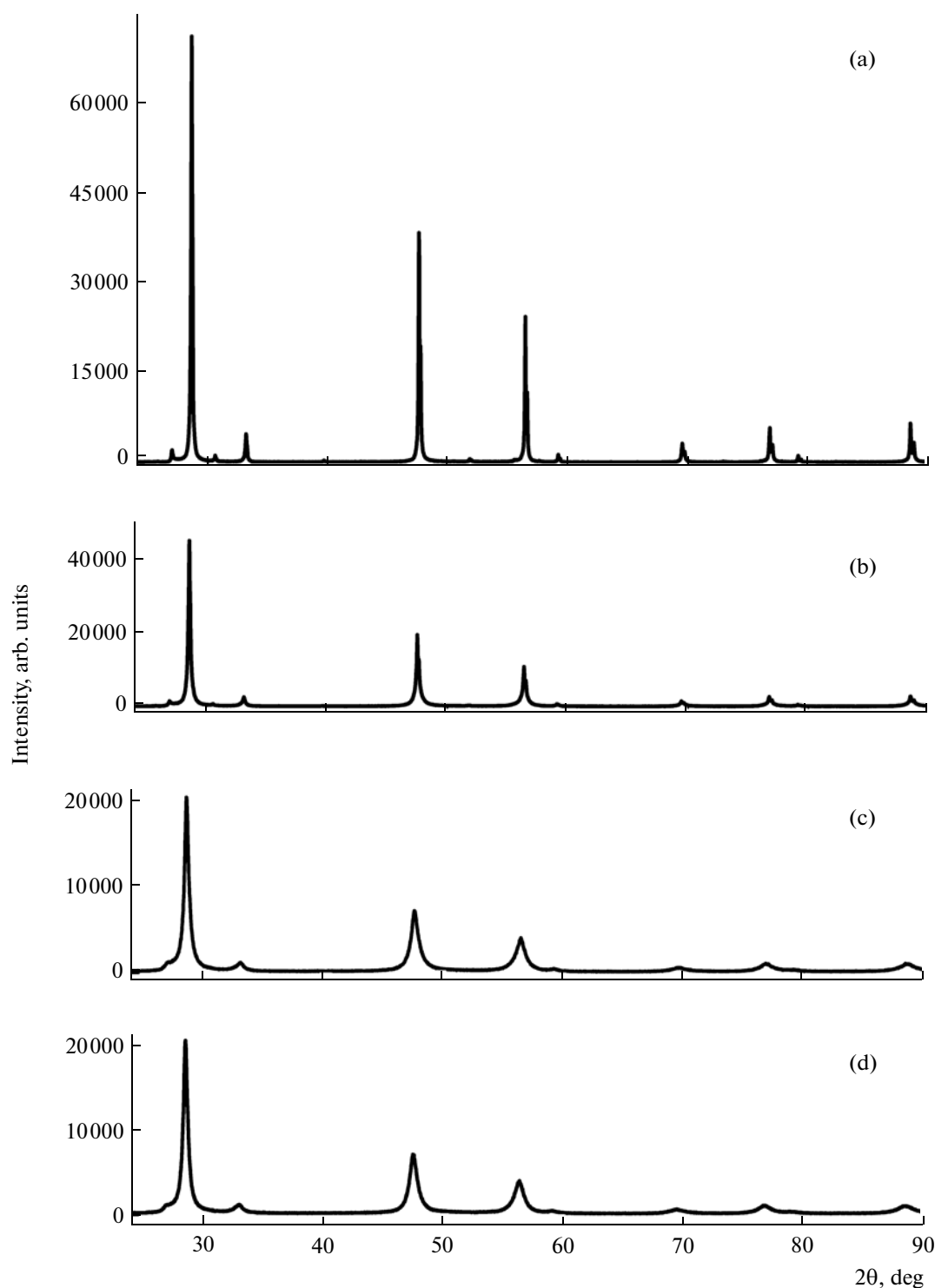


Fig. 1. X-ray diffraction patterns of $\text{Zn}_2\text{SiO}_4\text{:Mn}$ (willemite) powders before (a) and after milling for 15 (b), 60 (c), and 240 min (d).

dard Reference Powder 660a) with a lattice parameter $a = 415.69$ pm. The angular dependence of the full width at half maximum of a diffraction peaks, $FWHM_R$, was represented by an equation proposed by Rietveld [9]. The average particle size (crystallite size) $\langle D \rangle$ and lattice strain were evaluated using the Will-

iamson–Hall method [6, 10] to separate the particle size and strain contributions to diffraction line broadening.

The microstructure of the parent willemite and the powders milled for 120 and 240 min was also examined by scanning electron microscopy (SEM) on a Zeiss

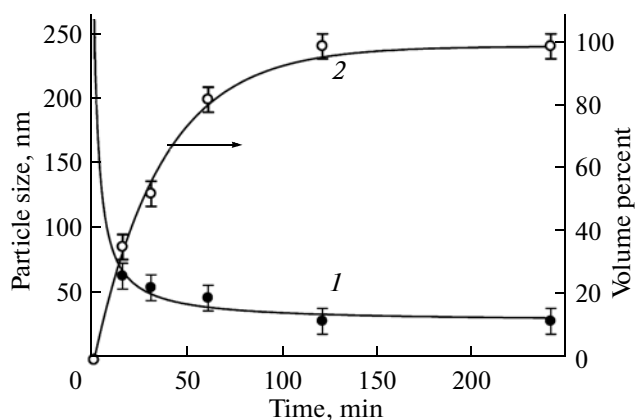


Fig. 2. Measured (1) average size (filled data points) and (2) volume percentage (open data points) of nanoparticles as functions of milling time for $\text{Zn}_2\text{SiO}_4\text{:Mn}$ powders.

Sigma VP instrument. Since $\text{Zn}_2\text{SiO}_4\text{:Mn}$ is a nonconductive material, the powders were applied to adhesive conductive adhesive tape and covered with a 10-nm-thick gold layer, which had no effect on the powder morphology and enabled quality SEM micrographs to be obtained.

Preliminary characterization of the microcrystalline $\text{Zn}_2\text{SiO}_4\text{:Mn}$ showed that the average particle size of the powder was 3 μm . In addition, the material had a strong tendency to agglomerate and, as a consequence, the powders contained particles up to 10 μm in size, consisting of several smaller crystals.

RESULTS AND DISCUSSION

Figure 1 shows X-ray diffraction patterns of the willemite powders before and after milling. Intrinsic

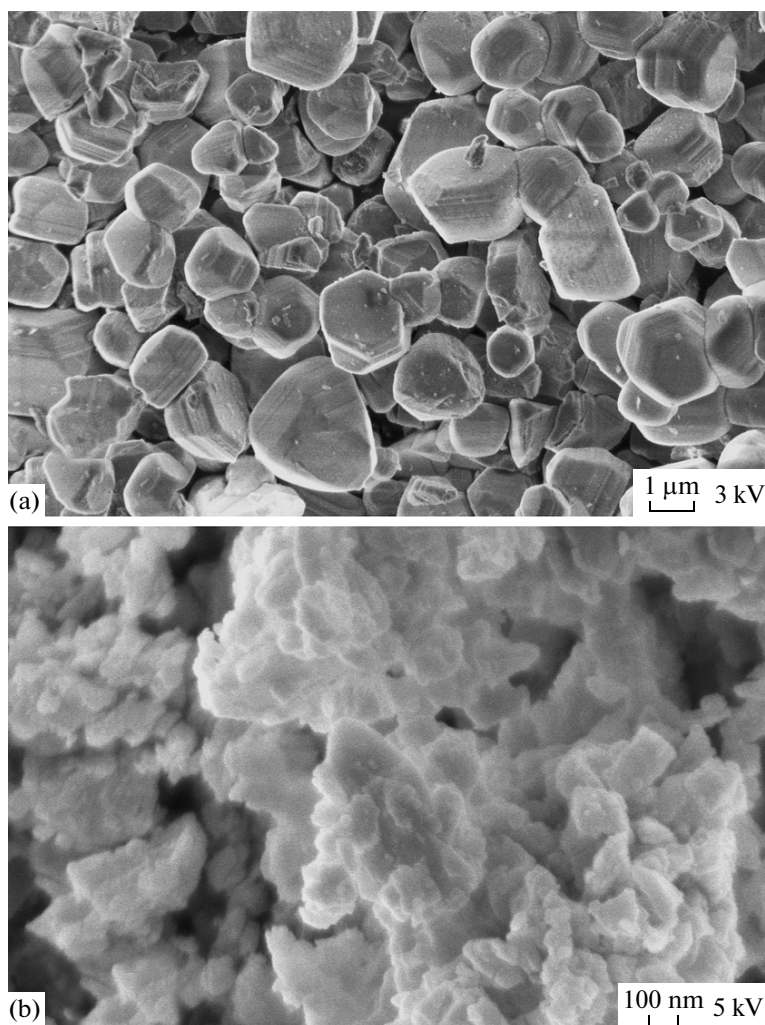


Fig. 3. SEM micrographs of $\text{Zn}_2\text{SiO}_4\text{:Mn}$ (willemite) powders: (a) unmilled microcrystalline powder with a particle size in the range 1–3 μm ; (b) powder milled for 240 min and consisting of nanoparticles 30 ± 10 nm in size, forming agglomerates about 400 nm in size.

broadening of diffraction peaks was observed after just 15 min of milling, but the sample still contained a large percentage of microcrystalline particles. The contents of micro- and nanocrystalline (less than 100 nm in size) particles in the milled powders were quantitatively estimated from the relative contributions of size fractions to the total intensity of diffraction peaks.

Figure 2 shows the volume percentage of nanoparticles as a function of milling time. The percentage of small particles is seen to rapidly decrease with increasing milling time, and after just 120 min the powder contains no large, unbroken particles. The data were fitted by an exponential function,

$$V(\tau) = a/(1 - \exp(-\tau/\tau_0))$$

with $a = 100\%$ and $\tau_0 = 35.71$ min.

According to calculation results, the average particle size of the small size fraction in the powders milled for 15, 30, and 60 min was 65 to 45 nm, and the average error of determination was ± 10 nm. Since those powders were not annealed, their lattice strain reached 0.98%. The particle size of the powders milled for 120 and 240 min was 30 ± 10 nm, and annealing markedly reduced the lattice strain in those powders, to 0.68%. Figure 2 shows the average particle size as a function of milling time.

The experimental particle size versus milling time data are well represented by a simple hyperbolic function,

$$D(\tau) = d_0 + a/(1 + b\tau),$$

proposed by Valeeva et al. [6], with $d_0 = 29.7$ nm, $a = 240.3$, and $b = 0.34 \text{ min}^{-1}$. Figure 2 demonstrates that the particle size of the powders rapidly decreases after just 15 min of milling and that milling for more than 240 min causes no further particle size reduction.

The SEM micrograph of the parent microcrystalline willemite in Fig. 3a shows rounded particles with a layered inner structure. The average particle size is 1–3 μm . In addition, there are agglomerates formed by several intergrown particles. It follows from Fig. 3b that the particles of the willemite milled for 240 min form agglomerates ranging in size from 100 to 400 nm, which in turn consist of finer particles, 30–50 nm in size.

CONCLUSIONS

Willemite powders down to 30 ± 10 nm in size have been prepared by ball milling. Luminescence studies

of the $\text{Zn}_2\text{SiO}_4\text{:Mn}$ nanopowders are planned to assess their potential for practical application as efficient cathodoluminescent phosphors.

ACKNOWLEDGMENTS

This work was supported in part by the Ural Branch and Presidium of the Russian Academy of Sciences (project no. 12-P-234-2003, program no. 24: Fundamental Issues in Technologies of Nanostructures and Nanomaterials).

REFERENCES

1. Zachariasen, W.H., Notizüber die Krystalstruktur von Phenakite, Willemite und verwandten Verbindungen, *Norsk Geol. Tidsskrift*, 1926, vol. 9, pp. 65–73.
2. Simonov, M.A., Sandomirskii, P.A., Egorov-Tismenko, Yu.K., and Belov, N.V., Crystal structure of willemite, Zn_2SiO_4 , *Dokl. Akad. Nauk SSSR*, 1977, vol. 237, no. 3, pp. 581–584.
3. Warner, T.E., *Synthesis, Properties and Mineralogy of Important Inorganic Materials*, Wiley, 2011, p. 211.
4. Klassen, H.V., Kedrov, V.V., Shmurak, S.Z., et al., New radiation-hard devices for ionizing radiation monitoring and direct radiation conversion to electrical energy based on nanostructured materials, *Yad. Izmer.-Inform. Tekhnol.*, 2011, vol. 38, no. 4, pp. 36–41.
5. Gal'china, N.A., Kogan, L.M., Soshchin, N.P., et al., Electroluminescence spectra of ultraviolet light-emitting diodes based on p - n InGaN/AlGaN/GaN heterostructures coated with phosphors, *Semiconductors*, 2007, vol. 41, no. 9, pp. 1143–1148.
6. Valeeva, A.A., Schroettner, H., and Rempel, A.A., Preparation of Nanocrystalline VO_y by High-Energy Ball Milling, *Inorg. Mater.*, 2011, vol. 47, no. 4, pp. 408–411.
7. Kurlov, A.S. and Gusev, A.I., Model for milling of powders, *Tech. Phys.*, 2011, vol. 81, no. 7, pp. 975–980.
8. Rempel, A.A., Nanotechnologies, properties, and applications of nanostructured materials, *Usp. Khim.*, 2007, vol. 76, no. 5, pp. 474–500.
9. Rietveld, H.M., A profile refinement method for nuclear and magnetic structures, *Appl. Crystallogr.*, 1969, vol. 2, no. 2, pp. 65–71.
10. Williamson, G.K. and Hall, W.H., X-ray line broadening from filed aluminium and wolfram, *Acta Metall.*, 1953, vol. 1, no. 1, pp. 22–31.

Translated by O. Tsarev